Petroleum and Coal

Article **Open Access**

Seismic and Petrophysical Characterization of Reservoirs in Kjoe Field, On-Shore Niger Delta, Nigeria

Kenechi Junior Obimma[1], Daniel N. Obiora[1,], Andrew I. Oha[2], Johnson C. Ibuot[1], John A. Yakubu[1]*

[1] Department of Physics and Astronomy, University of Nigeria, Nsukka, Enugu State, Nigeria
[2] Department of Geology, University of Nigeria, Nsukka, Enugu State, Nigeria

Received August 16, 2020; Revised November 23, 2020, Accepted December 21, 2020

Abstract

Integrated seismic reservoir characterization (ISRC) approach was used to merge seismic and petrophysical analysis to characterize potential hydrocarbon reservoirs present in "KJOE field", on-shore, Niger-Delta, Nigeria. Available data used include suites of six well logs with petrophysical logs (GR log, resistivity log, neutron and density logs), check shot, deviation and reservoir tops and bottom data to enable appropriate characterization with post-stacked seismic data which provides the structural seismic analysis for the study area. The lithologies were identified and correlated in the well section and petrophysical properties were determined to show that the reservoir sands (E1000, E2000, E3000, E4000, E4500, E5000, E6000, E7000, E8000 and F2000) have outstanding petrophysical characteristics. The reservoirs ranging from 3.62 m to 42.97 m gross thickness contain between 2.50% to 24.30% volumes of unconsolidated shale with a considerably better sand quality. On average, these reservoirs have a hydrocarbon saturation of about 13.10% to 99.30% with permeability values of 15.9483 md to 56.8873 md. Well KJOE 08 generally contains water with Bulk Volume of Water ranging from 0.2033 to 0.2539 and high water saturation values of about 95.80% to 99.80%. Depth structure maps were generated and interpreted to show that the field has three growth faults (F2, F3, F5) trending from the northeast to southwest direction and enhances the trapping of hydrocarbon in this field. Synthetic seismogram was used to create a well to-seismic tie.

***Keywords**: Integrated seismic reservoir characterization; Hydrocarbon reservoir; Seismic data; Petrophysical analysis; Niger Delta.*

1. Introduction

All hydrocarbon exploration projects have the common goal of finding reserves of oil and gas that are profitable. It is well known that finding these new hydrocarbon reserves is very expensive and there is need to use less expensive method to detect and quantify these reservoirs with reduced level of uncertainty associated with geological models. Reservoir characterization is a process of describing various reservoir characteristics using all available data to provide reliable reservoir models for accurate reservoir performance prediction. Initial understanding of the reservoir properties (porosity, permeability, water saturation, thickness, and area extent of the reservoir) is crucial in determining hydrocarbon potential of any basin because they serve as necessary and important inputs for reservoir volumetric/economic analysis [1]. Identification of lithologies like sandstones is done with the help of Gamma ray log. Also Gamma ray logs can be used to identify other lithologies like limestone and dolomites if core data exist. The resistivity log differentiates between water and hydrocarbon in the pore space of the reservoir rocks. It is used to obtain the true formation resistivity and to identify the oil-water contact [2].

Hydrocarbons are found in geologic traps and these traps can either be structural, stratigraphic or a combination of both. According to [3], majority of traps in the Niger Delta are structural. To locate these traps for the hydrocarbon accumulations, faults and horizons are mapped on the section to produce the structure maps. This study tries to use 3D seismic reflection data obtained in the KJOE field to delineate the lithologies, locate structural traps by mapping the faults and horizons and making the structure maps used in identifying the hydrocarbon bearing reservoir. Some studies have been carried out in different locations in the Niger Delta [1,4-6].

2. Location and geology of the study area

The KJOE oilfield, situated in the Central Swamp I Depo-Belt of the Niger Delta (Figure 1), is owned and managed by Shell Petroleum Development Company (SPDC) Nigeria Limited concession. The Niger Delta (Figure 2) is an upward-coarsening regressive association of Tertiary clastics with thickness up to 12*Km* or 39370ft and is divided into three gross lithofacies [3, 7-9]:

(i) Benin Formation (Continental Sands): This is the youngest lithostratigraphic unit with a minimum thickness of more than 6,000 ft (1,829 m) and made up of continental sands and sandstones of up to 90% in formation with few shale intercalations.

(ii) Agbada Formation (Paralic Clastics): According to [10] and [11], this formation with a thickness of over 9842.5 ft (3,000 m) is characterized by paralic interbedded sandstone and shale. It forms the hydrocarbon-prospective sequence and most exploration wells are sited here.

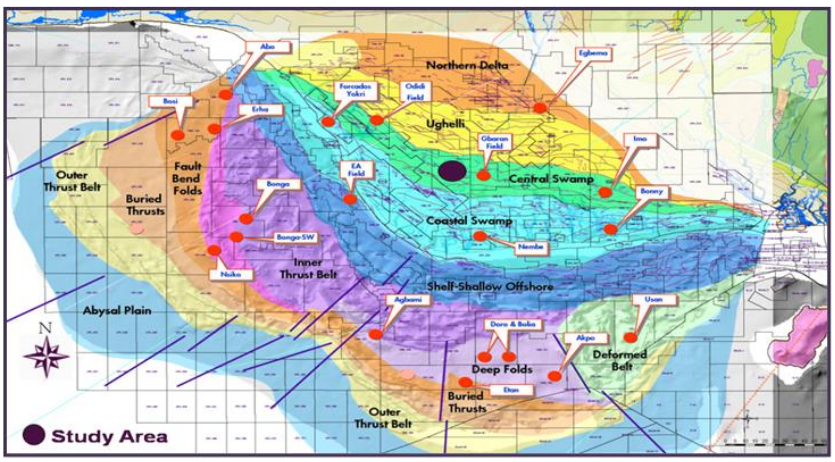

Fig. 1. Structural play segments, onshore and offshore Nigeria [12]

(iii) Akata Formation (Marine Shales): This is the oldest lithostratigraphic unit ranging from 1,968.5 to 19,685 ft (600 – 6,000 m) in thickness and consists of mainly uniform under-compacted shales, clays, and silts at the base of the known delta sequence with lenses of sandstone of abnormally high pressure at the top [9]. Ejedawe *et al.* [13] deduced that the shales of this formation are the main source rocks of the Niger Delta.

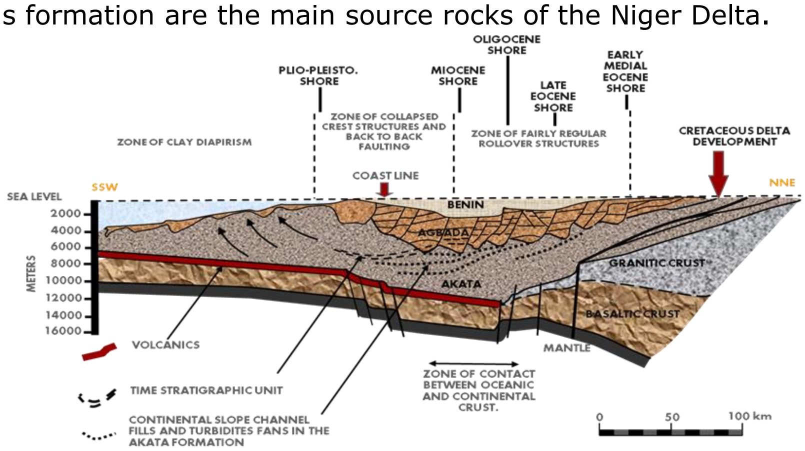

Fig. 2. Schematic Dip Section of the Niger Delta [14]

Virtually all the hydrocarbon found is in the paralic sand, trapped in rollover anticlines or against growth faults along footwall (Figure 3). Minor stratigraphic traps also occur in some fields due to lateral facies changes or in association with clay- filled channels [15].

Edwards *et al.* [16] described the primary Niger Delta reservoirs as Miocene paralic sandstones with 40% porosity, 2000 millidarcys permeability and thickness of 100metres. Weber *et al.* [14] described the lateral variation in the thickness of the reservoir to be strongly controlled by growth faults and the reservoir grows thicker towards the fault within the downthrown block.

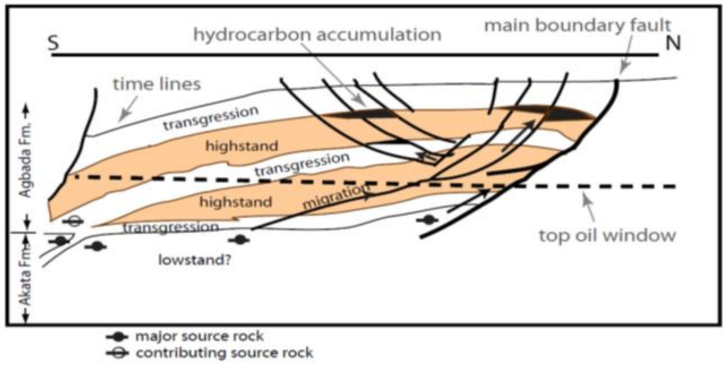

Fig.3. Sequence stratigraphic model for the central portion of the Niger Delta showing the relation of source rock, migration pathways and hydrocarbon traps related to growth faults [17]

The primary aim of this work is to integrate 3-D seismic and petrophysical data for the characterization of KJOE field, Niger Delta in order to (i) correlate and map the E-sand distributions across the field, (ii) estimate the petrophysical parameters of the KJOE Field from the well logs and (iii) generate time and depth structure maps of the E-horizons for structural analysis.

3. Source of data

The dataset used in this work gotten from KJOE oilfield were obtained from Shell Petroleum Development Company (SPDC), Nigeria. The dataset includes suites of thirteen well logs (spread between surface X-coordinate of 499486.34 m and 510953.88 m easting to surface Y-coordinate of 56351.14 m and 58851.91 m northing) and a three-dimensional (3D) post-stacked seismic data (covering an area between surface X-coordinate of 498726.50 m and 515551.50 m easting to surface Y-coordinate of 52433.50 m and 63058.50 m northing). Generally, the well logs which contain check shot data, deviation data and reservoir tops and bottom data, span to a depth of 14916 ft (4546.40 m) from the ground surface while the seismic data, with both inline and crossline interval of 25.00 has 673 inlines and 425 crosslines. This acquired data set were validated, analyzed and interpreted using the 2011 version of Schlumberger Petrel software and Interactive Petrophysics software (Version 3.1.0.9).

4. Method of analysis

The main physical parameters (lithologies, formation thickness, porosity, permeability, water saturation, etc.) necessary for reservoir characterization are usually derived from log signatures. Gamma ray log is used in calculating volume of shale due to its radioactive characteristics.

Volume of shale, V_{SH}, for unconsolidated rocks [18] in any reservoir is calculated using:

$$V_{SH} = 0.083\left[2^{(3.7 \times I_{GR})} - 1.0\right] \qquad (1)$$

where I_{GR} (gamma ray index), according to [2] given as:

$$I_{GR} = \frac{GR_{log}-GR_{min}}{GR_{max}-GR_{min}} \qquad (2)$$

where GR_{log} = Gamma Ray reading from the gamma ray log; GR_{min}= Minimum Gamma Ray of a relatively clean sand formation and GR_{max}= Maximum Gamma Ray of an adjacent shale formation

The porosity of a reservoir rock, defined as the fraction of the bulk volume that is not occupied by the solid framework of the rock, that is, pore space, is usually calculated using the porosity (neutron and density) logs. Effective porosity value is obtained using

$$\phi = \phi_{N\text{-}D} + (1 - V_{sh}) \qquad (3)$$

where $\phi_{N\text{-}D}$ = neutron-density derived porosity given by:

$$\phi_{N\text{-}D} = \frac{\sqrt{\phi_N^{\,2} + \phi_D^{\,2}}}{2} \qquad (4)$$

and ϕ_N is the porosity from neutron log read straight from the neutron log and ϕ_D is the porosity from density log obtained by [18] as:

$$\phi_D = \frac{\rho_{ma} - \rho_b}{\rho_{ma} - \rho_f} \qquad (5)$$

where ρ_{ma} is the matrix density obtained from header of density log (g/cm^3); ρ_b is the bulk density read from the density log (g/cm^3) and ρ_f is the fluid density obtained from header of density log (g/cm^3).

Net-to-Gross Ratio (NGR) is a measure of the proportion of clean sand within a reservoir unit and which reflects the quality of the sands as potential reservoirs, is calculated using:

$$\text{Net-to-Gross Ratio, NGR} = \frac{\text{Net sand}}{\text{Gross sand}} \qquad (6)$$

Water Saturation, which is the extent to which the pore space is filled with water, is calculated for an uninvaded zone using Archie's equation [19]:

$$S_W = \left(F \text{ x } \frac{R_w}{R_t}\right)^{\frac{1}{n}} \qquad (7)$$

where R_t is the true formation resistivity (uninvaded zone from Resistivity log); R_w (water resistivity) = 0.04Ωm; n is the saturation exponent usually taken as 2.0 and F is the formation factor given by Humble's formula proposed as [19]:

$$F = \frac{a}{\phi^m} = \frac{0.62}{\phi^{2.15}} \qquad (8)$$

where a = tortousity value = 0.62 and m = cementation factor = 2.15 as modified by [19].

Finally, Hydrocarbon saturation can be calculated using:

$$S_H = 1 - S_W \qquad (9)$$

The bulk volume of water, BVW is calculated using [20]:

$$BVW = S_w \text{ x } \phi \qquad (10)$$

The permeability of a reservoir rock may be defined as its fluid conductivity or ability to allow fluid flow within its interconnected pore network. It is measured in darcys or millidarcys (md) and calculated using the Timur's equation [21]:

$$K = \frac{0.136 \text{ x } \phi^{4.4}}{S_{wirr}^{\,2}} \qquad (11)$$

where S_{wirr} is the irreducible water saturation, given by [22] as;

$$S_{wirr} = \sqrt{\frac{F}{2000}} \qquad (12)$$

Also, the various contacts such as Gas-Oil Contact (GOC), Oil-Water Contact (OWC), Gas-Down-To (GDT) and Oil-Up-To (OUT) were derived from the combined analysis of these three logs**.** The determination of the reservoir geometry and understanding of the geologic history while locating its structures were carried out using seismic interpretation, which assumes that coherent events on seismic section are difference in acoustic impedance [23]. This contrast denotes different geologic features. To understand the field's subsurface geology, a 3D seismic data is displayed alongside the well tops in order to map out structures like faults and horizons of interest. Synthetic seismogram was adopted in tying well log to seismic data in this research. Major faults were identified and mapped along the dip lines, named and colour-coded for easy identification. Based on the horizon marked, care was taken in consistently delineating fault traces as faults are prone to die out and can be mistaken for similar one in a field with complex faulting system. After picking out the faults and horizons, Time and Depth structural maps were created for each horizon for structural analysis.

5. Results and interpretation

Six (6) well logs (KJOE 05, KJOE 07, KJOE 08, KJOE 09, KJOE12R and KJOE 13) were selected from the whole thirteen (13) well logs based on their horizontal ground position and compactness with one another towards a certain region of the surveyed field (Figure 4).

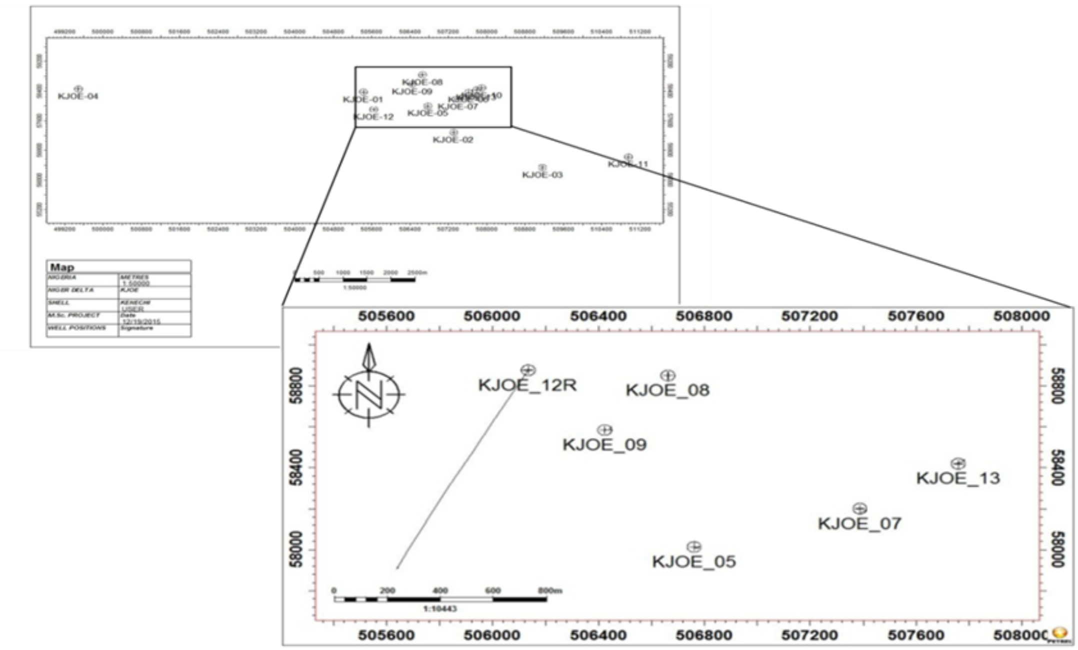

Fig. 4. Map Window of the six (6) selected wells

These logs were viewed and then interpreted to determine the various lithologies as whether sand and shale zones (Figure 5). Tables 1 – 10 show the summary of the petrophysical data obtained from the selected well logs on the study area.

Table 1. Petrophysical properties of E1000 reservoir sand across the selected wells

Wells	Reservoir thickness (ft)	Net-to-gross ratio	Volume of Shale V_{SH}(%)	Porosity ϕ	Water Saturation S_W(%)	Bulk Volume of water (BVW)	Permeability K, (md)	Predominant type of hydrocarbon
KJOE 05	134.07	0.1360	10.30	0.2430	8.70	0.0211	41.4857	Gas
KJOE 07	119.60	0.4310	12.30	0.2460	1.30	0.0032	44.9575	Gas
KJOE 08	119.92	0.9510	15.60	0.2300	99.80	0.2295	28.9397	Water
KJOE 09	140.97	0.2060	12.00	0.2430	8.50	0.0207	41.4857	Gas
KJOE 12	130.18	1.0000	2.50	0.2550	14.50	0.0370	56.8873	Oil
KJOE 13	100.87	0.4950	10.70	0.2410	8.60	0.0207	39.2997	Gas

Table 2. Petrophysical properties of E2000 reservoir sand across the selected wells

Wells	Reservoir thickness (ft)	Net-to-gross ratio	Volume of Shale V_{SH}(%)	Porosity ϕ	Water Saturation S_W(%)	Bulk Volume of water (BVW)	Permeability K, (md)	Predominant type of hydrocarbon
KJOE 05	60.41	0.5480	8.60	0.2510	86.90	0.2181	51.2909	Oil & water
KJOE 07	55.03	0.8030	11.50	0.2340	0.70	0.0016	32.3997	Oil
KJOE 08	58.55	0.9140	18.40	0.2440	99.30	0.2423	42.6168	Water
KJOE 09	53.24	0.1790	15.80	0.2350	12.70	0.0298	33.3174	Oil
KJOE 12	48.26	0.6530	3.60	0.2450	15.90	0.0390	43.7739	Oil
KJOE 13	43.63	0.7130	12.30	0.2300	6.60	0.0152	28.9397	Oil

Table 3. Petrophysical properties of E3000 reservoir sand across the selected wells

Wells	Reservoir thickness (ft)	Net-to-gross ratio	Volume of Shale V_{SH}(%)	Porosity ϕ	Water Saturation S_W(%)	Bulk Volume of water (BVW)	Permeability K, (md)	Predominant type of hydrocarbon
KJOE 05	15.28	0.7590	8.20	0.2370	100.00	0.2370	35.2192	Water
KJOE 07	59.96	0.5050	11.00	0.2240	1.80	0.0040	24.3389	Oil
KJOE 08	62.55	0.9760	15.20	0.2460	99.30	0.2443	44.9575	Water
KJOE 09	47.80	0.5380	13.90	0.2450	8.50	0.0208	43.7739	Oil
KJOE 12	50.65	0.8640	4.20	0.2370	17.60	0.0417	35.2192	Oil
KJOE 13	61.67	0.6640	15.20	0.2150	9.00	0.0194	18.6058	Oil

Table 4. Petrophysical properties of E4000 reservoir sand across the selected wells

Wells	Reservoir thickness (ft)	Net-to-gross ratio	Volume of Shale V_{SH}(%)	Porosity ϕ	Water Saturation S_W(%)	Bulk Volume of water (BVW)	Permeability K, (md)	Predominant type of hydrocarbon
KJOE 05	-	-	-	-	-	-	-	-
KJOE 07	11.89	0.8040	12.10	0.2450	3.90	0.0096	43.7739	Oil
KJOE 08	15.28	0.8150	16.40	0.2400	99.20	0.2381	38.2438	Water
KJOE 09	25.79	0.9100	12.80	0.2540	33.20	0.0843	55.4419	Oil & water
KJOE 12	37.11	0.9650	6.00	0.2320	75.80	0.1759	30.6283	Oil & water
KJOE 13	15.40	0.5320	15.70	0.2110	15.80	0.0333	16.4523	Oil

Table 5. Petrophysical properties of E4500 reservoir sand across the selected wells

Wells	Reservoir thickness (ft)	Net-to-gross ratio	Volume of Shale V_{SH}(%)	Porosity ϕ	Water Saturation S_W(%)	Bulk Volume of water (BVW)	Permeability K, (md)	Predominant type of hydrocarbon
KJOE 05	-	-	-	-	-	-	-	-
KJOE 07	91.41	0.7440	8.50	0.2400	56.10	0.1346	38.2438	Water
KJOE 08	19.18	1.0000	15.70	0.2650	95.80	0.2539	73.1876	Water
KJOE 09	20.67	0.8000	11.60	0.2200	98.90	0.2176	21.6295	Water
KJOE 12	34.53	0.9350	7.90	0.2480	97.60	0.2420	47.4063	Water
KJOE 13	94.45	0.5910	12.80	0.2100	9.80	0.0206	15.9483	Oil

Table 6. Petrophysical properties of E5000 reservoir sand across the selected wells

Wells	Reservoir thickness (ft)	Net-to-gross ratio	Volume of Shale V_{SH}(%)	Porosity ϕ	Water Saturation S_W(%)	Bulk Volume of water (BVW)	Permeability K, (md)	Predominant type of hydrocarbon
KJOE 05	-	-	-	-	-	-	-	-
KJOE 07	47.59	0.8560	10.70	0.2370	50.50	0.1197	35.2192	Water
KJOE 08	63.15	0.9360	18.70	0.2390	99.00	0.2366	37.2120	Water
KJOE 09	-	-	-	-	-	-	-	-
KJOE 12	80.68	0.9180	5.50	0.2520	97.00	0.2444	52.6442	Water
KJOE 13	49.17	0.7630	11.20	0.2350	80.80	0.1899	33.3174	Oil & water

Table 7. Petrophysical properties of E6000 reservoir sand across the selected wells

Wells	Reservoir thickness (ft)	Net-to-gross ratio	Volume of Shale V_{SH}(%)	Porosity ϕ	Water Saturation S_W(%)	Bulk Volume of water (BVW)	Permeability K, (md)	Predominant type of hydrocarbon
KJOE 05	-	-	-	-	-	-	-	-
KJOE 07	-	-	-	-	-	-	-	-
KJOE 08	127.69	0.8940	24.30	0.2270	99.00	0.2247	26.5550	Water
KJOE 09	-	-	-	-	-	-	-	-
KJOE 12	45.77	0.9270	7.70	0.2530	95.70	0.2421	54.0277	Water
KJOE 13	39.78	0.5320	12.60	0.2140	100.00	0.2140	18.0463	Water

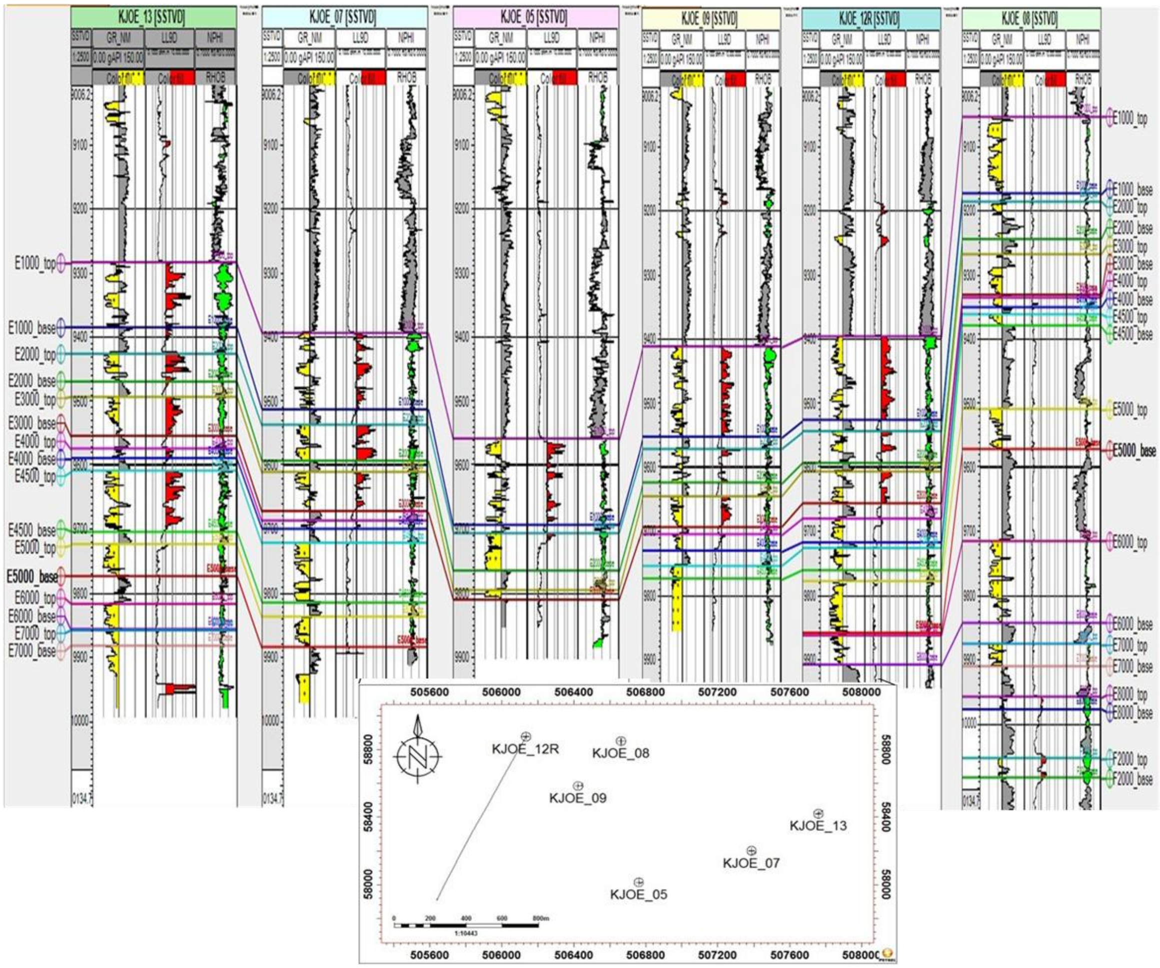

Fig. 5. Interpretation Window showing the selected six (6) well logs displaying the gamma, resistivity and neutron-density log signatures with map Window of the six selected wells attached

Table 8. Petrophysical properties of E7000 reservoir sand across the selected wells

Wells	Reservoir thickness (ft)	Net-to-gross ratio	Volume of Shale V_{SH}(%)	Porosity ϕ	Water Saturation S_W(%)	Bulk Volume of water (BVW)	Permeability K, (md)	Predominant type of hydrocarbon
KJOE 05	-	-	-	-	-	-	-	-
KJOE 07	-	-	-	-	-	-	-	-
KJOE 08	34.42	0.9560	14.80	0.2060	98.70	0.2033	14.0607	Water
KJOE 09	-	-	-	-	-	-	-	-
KJOE 12	-	-	-	-	-	-	-	-
KJOE 13	23.54	0.2390	16.50	0.2110	100.00	0.2110	16.4523	Water

Table 9. Petrophysical properties of E8000 reservoir sand across the selected wells

Wells	Reservoir thickness (ft)	Net-to-gross ratio	Volume of Shale V_{SH}(%)	Porosity ϕ	Water Saturation S_W(%)	Bulk Volume of water (BVW)	Permeability K, (md)	Predominant type of hydrocarbon
KJOE 05	-	-	-	-	-	-	-	-
KJOE 07	-	-	-	-	-	-	-	-
KJOE 08	18.10	1.0000	12.20	0.2670	22.40	0.0598	76.8822	Oil
KJOE 09	-	-	-	-	-	-	-	-
KJOE 12	-	-	-	-	-	-	-	-
KJOE 13	-	-	-	-	-	-	-	-

Table 10. Petrophysical properties of F2000 reservoir sand across the selected wells

Wells	Reservoir thickness (ft)	Net-to-gross ratio	Volume of Shale V_{SH}(%)	Porosity ϕ	Water Saturation S_W(%)	Bulk Volume of water (BVW)	Permeability K, (md)	Predominant type of hydrocarbon
KJOE 05	-	-	-	-	-	-	-	-
KJOE 07	-	-	-	-	-	-	-	-
KJOE 08	30.73	0.8690	14.20	0.2610	17.10	0.0446	66.2480	Gas
KJOE 09	-	-	-	-	-	-	-	-
KJOE 12	-	-	-	-	-	-	-	-
KJOE 13	-	-	-	-	-	-	-	-

From the results obtained, the reservoir sands occurring at subsea true vertical depth (SSTVD) ranging from −9052.47 ft (−2759.19 m) to −10083.98 ft (−3109.90 m) have outstanding petrophysical properties. The gross thickness of the reservoirs ranges from 11.89 ft (3.62 m) to 140.97 ft (42.97 m), containing between 2.50% to 24.30% volumes of unconsolidated shale. The net to gross ratio calculated for all reservoirs ranges from 0.1360 to 1.0000 while hydrocarbon prone reservoirs were discovered to have a considerably high values indicating better sand quality with hydrocarbon saturation of about 13.10% to 99.30% and permeability values of 15.9483 md to 56.8873 md. For well KJOE 08, contents in the reservoirs E1000 to E7000 is generally water with high water saturation values of about 95.80% to 99.80%.

The log signatures show that reservoirs in all the selected wells have contact types to be mainly oil-down-to (ODT) and oil-up-to (OUT) except for well KJOE 08. There was at least two (2) gas-down-to (GDT) and gas-up-to (GUT) present in each surveyed wells: KJOE 07, KJOE 09 and KJOE 13 while reservoirs in well KJOE 12 have neither gas-down-to (GDT) nor gas-up-to (GUT) present in it. Only one (1) gas-oil contact (GOC) was found in reservoirs of the KJOE 05 and KJOE 09 wells and also one (1) oil-water contact (OWC) was found in those of wells KJOE05, KJOE09, KJOE 12R and KJOE 13.

5.1.Seismic interpretation

The time migrated and processed seismic sections reflect the true amplitude of events in the field. Overall appearance of reflection patterns is generally continuous except in areas with faults and marine shale. Based on the zones' absorption coefficient, positive amplitude within the section (red-coloured lines) represents sand while the negative amplitude (blue-coloured lines) represents shale formation (Figures 6 and 8). Changes in the behaviour of the amplitude reflect the exact subsurface condition; thus resolving the structural and stratigraphic nature of the field. To map out structures like faults and horizons of interest, conversion of well data from depth domain to time domain was carried out.

5.2. Well-to-seismic tie

From the control well (KJOE10), both density and sonic logs were used to create a synthetic seismogram for performing well to seismic tie. This seismogram lead to proper tie of well data properties to that of seismic which enabled the selection of the horizon on the post-stacked 3D seismic data.

Figure 6 showed that the E-sands and F2000 sand reservoirs were tied from the well to the post-stacked 3D seismic data at a time of 2320 to 2490 ms. Due to the above average predictability of 54.1%, horizon interpretation was approached and achieved. On the interpretation window of inline 6980 and crossline 1165 on the seismic data, the E1000, E3000 and E4000 sand reservoirs were marked at the 2320 ms, 2360 ms and 2375 ms positive amplitude (red coloured) lines respectively.

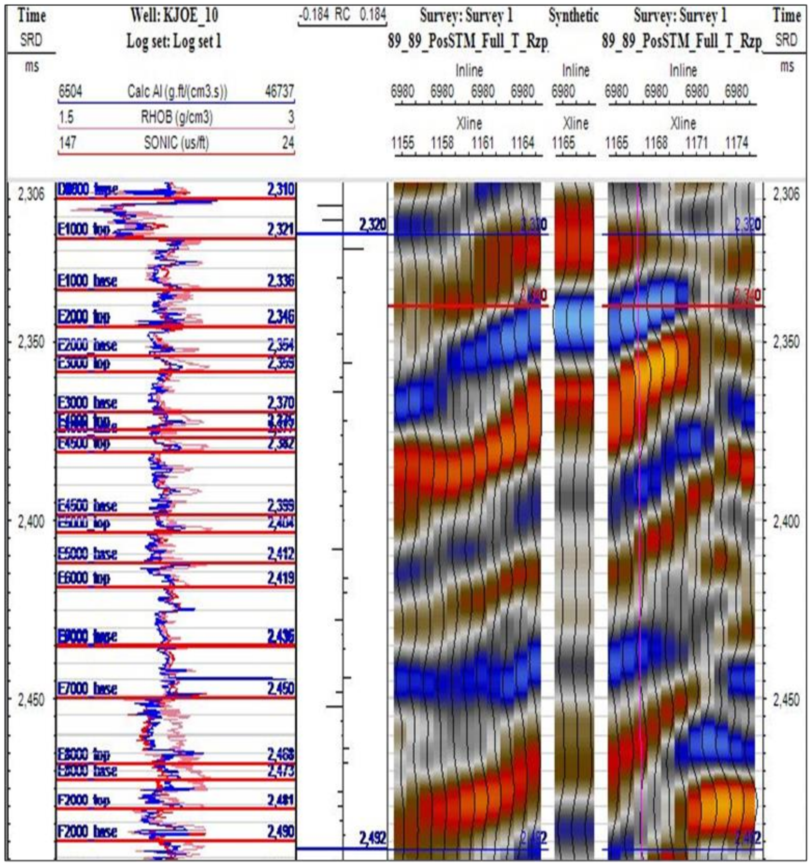

Fig. 6. Well to seismic tie using well KJOE 10

5.3. Fault interpretation

From the seismic section, it was observed that the field was complexly faulted. At 10 in-line interval, faults were picked, assigned names and identified with different colours in order to differentiate them on the seismic survey (Figures 8). After interpreting these faults on the entire survey, their respective fault polygons were picked, edited and modeled on a two–dimensional (2D) window.

This result (Figure 7) showed three major growth faults (F2, F3 and F5) with curved fault planes trending in the northeast to southwest direction. The top and centre growth faults, F2 and F3, have a smaller fault springing out from them in the same direction. These are faults F1 and F8 respectively.

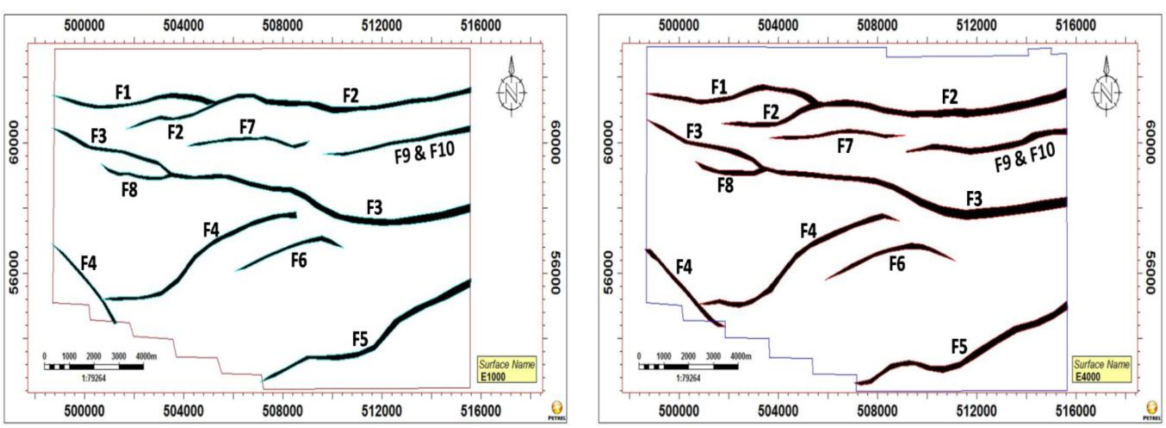

Fig. 7. Map view of the modeled faults on the E1000 and E4000 survey

5.4. Horizon interpretation

After establishing a tie between the available well data and seismic survey, horizon interpretation was carried out on the generated fault map. Three horizons (E1000, E2000 and E4000) were considered for interpretation (Figure 8) and viewed in the map window which enabled proper horizon mapping (Figure 9).

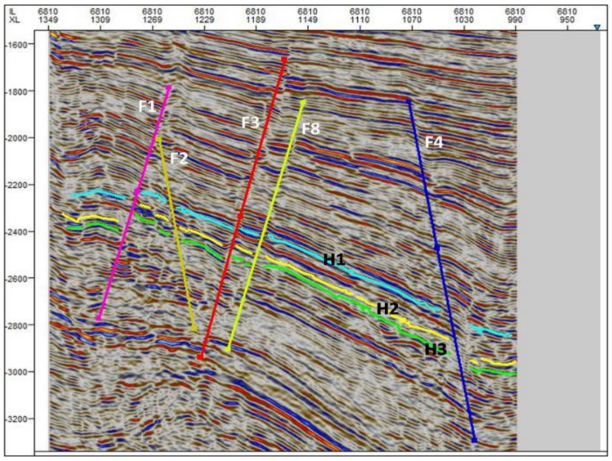

Fig. 8a. Interpreted Horizons on in-line 6810

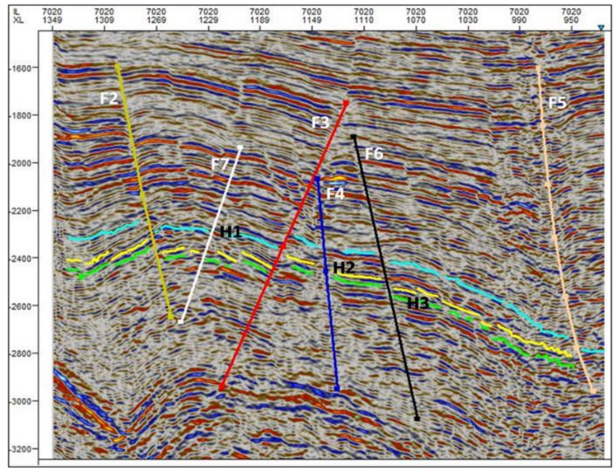

Fig.8b. Interpreted Horizons on in-line 702

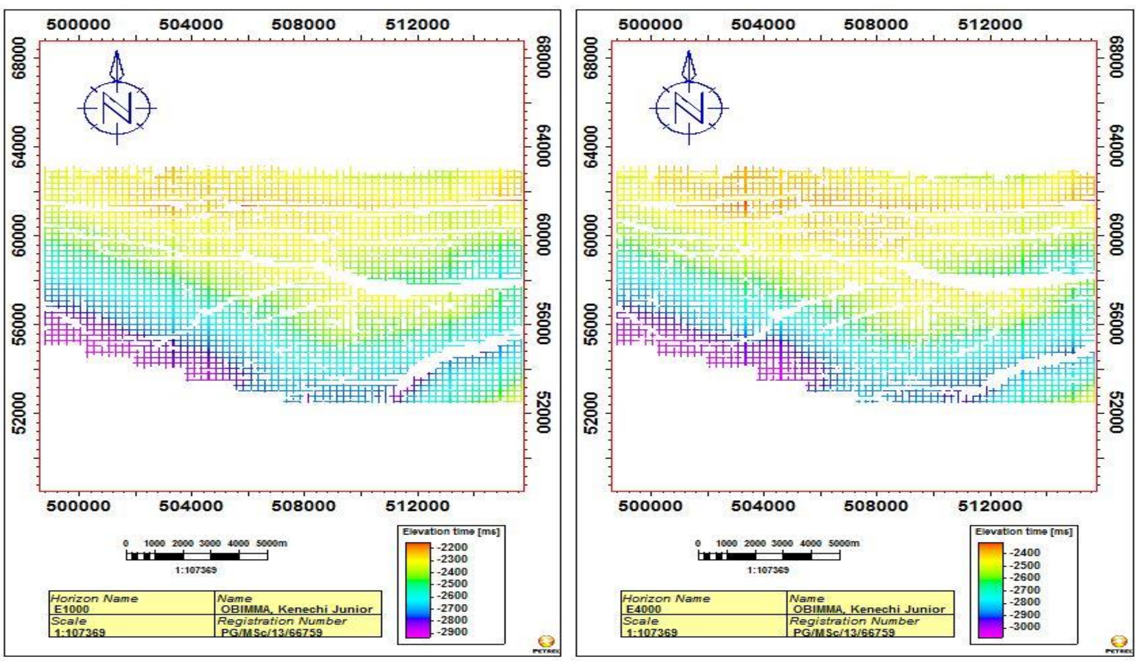

Fig. 9. Map view of E1000 and E4000 horizons

Time structure map (Figure 10) show the various structures associated with the field in the relationship with their time position. Time structure maps were produced for each of the reservoir's tops and were presented in contour interval of 20 ms with the maximum (top) and minimum (bottom) subsea contour values for the reservoirs as: 2200 ms and 2900 ms for E1000; 2300 ms and 3000 ms for E3000 and 2340 ms and 3060 ms for E4000.

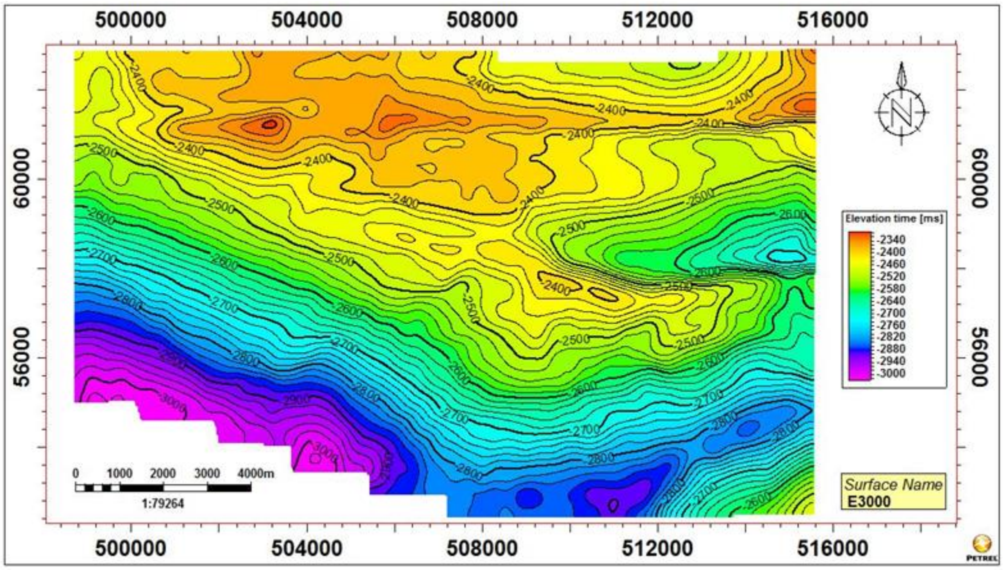

Fig. 10. Time structural map view of E3000

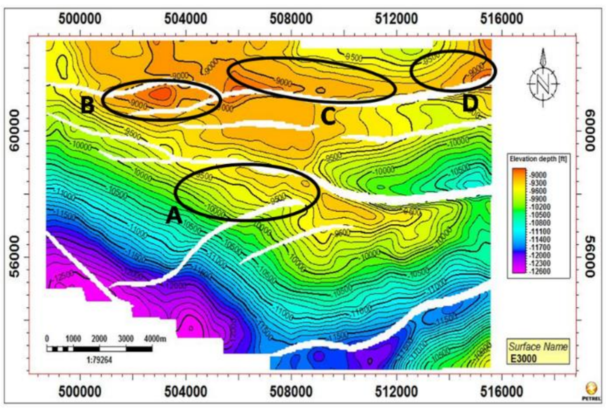

Fig. 11a. Depth structural map view of E1000

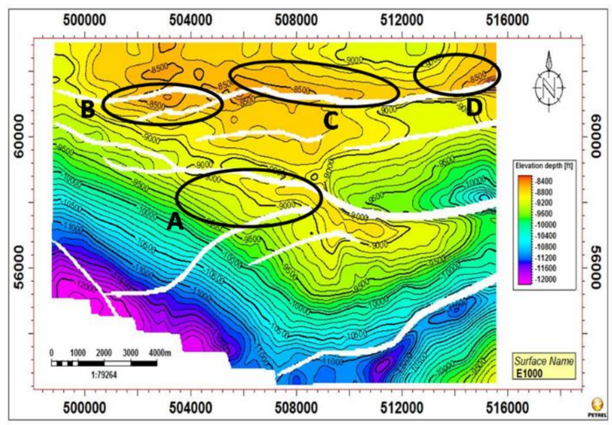

Fig. 11b. Depth structural map view of E3000

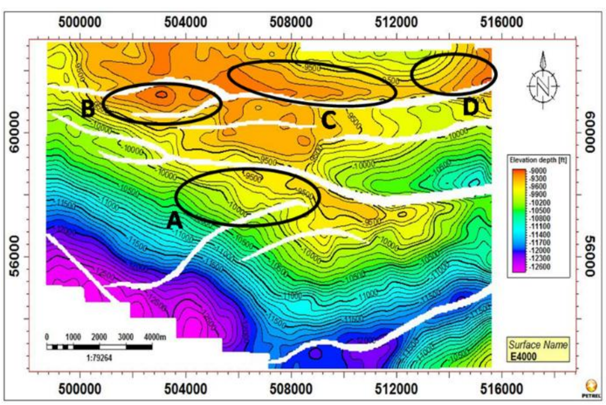

Fig. 11c. Depth structural map view of E4000

Depth structure maps, showing the various structures in relation with their depth in the field, were obtained from each of the time structural maps produced. These depth structural maps were created from the generated time structural maps using a time-depth (T-Z) polynomial created from a general checkshot data given in the data set. The different fault patterns were embedded into these maps to produce more detailed depth structural maps for each horizon. Presenting in contour interval of 100 ft (30.48 m), for example figure 11a-c, the reservoirs' maximum (top) and minimum (bottom) subsea contour depth values are: −8000 ft (−2438.40 m) and −12200 ft (−3718.56 m) for E1000 reservoir sand; −8700 ft (−2651.76 m) and −12600 ft (−3840.48 m) for E3000 sand and −8900 ft (−2712.72 m) and −12800 ft (−3901.44 m) for E4000 reservoir sand.

6. Conclusion

From the three dimensional view of the wells and seismic data, virtually all the hydrocarbon prospects found are in the paralic sands and trapped against growth faults along footwall. Wells KJOE 09 and KJOE 13 are partially deviated towards their ending along the depth axis. Well KJOE 12R is a side-tracked well which is highly deviated down into the earth's surface. Well KJOE 08 is situated on a growth fault which is why no hydrocarbon was detected since hydrocarbon migrates to stop at an enclosure.

Based on the petrophysical data, these reservoirs occur in sandstones with 21.00% to 26.70% porosity and thickness of 50*ft* (or 15.24*m*) except in the gas zones (E1000-sand) which have their average thickness as 120*ft* (or 36.58*m*). The lateral variation in the thickness of these reservoirs was randomly distributed, possibly due to multiple faults (F4 and F6) around the growth fault, F3.

Possible hydrocarbon prospects are identified as boxes labeled 'B' at the north-western part of the survey; 'C' at the northern part of the survey and 'D' at the north-eastern part of the survey. Prospect A has already spud wells where the petrophysical analysis were obtained.

Acknowledgement

The authors are grateful to Shell Petroleum Development Company (SPDC), Port Harcourt, for the data employed in this work. We thank the Editor-in-Chief and the reviewers for their meticulous work.

References

[1] Obiora DN, Gbenga D, and Ogobiri G. Reservoir Characterization and Formation Evaluation of a "Royal Onshore Field", Southern Niger Delta using Geophysical Well Log Data. Journal Geological Society of India, 2016; 87: 591-600.

[2] Schlumberger (1998) Log Interpretation Charts; Schlumberger Wireline and Testing. Sugar Land, Texas.

[3] Doust H, and Omatsola E. Niger Delta. In: J. D. Edwards, P. A. Santogrossi (Eds), Edition (Divergent and Passive margin Basins). American Association of Petroleum Geologists Memoir, 1990; 48: 201-238.

[4] Okwoli E, Obiora DN, Adewoye O, Chukudebelu JU, and Ezema PO. Reservoir characterization and volumetric analysis of "LONA" Field, Niger Delta, using 3-D seismic and well log data. Pet Coal, 2015; 57(2): 108-119.

[5] Emujakporue GO, and Faluyi TO. Evaluation of Hydrocarbon Volume in 'TRH' Field, Onshore Niger Delta, Nigeria. International Journal of Geophysics and Geochemistry, 2015; 2(5): 113-123.

[6] Adigwe P, and Inichinbia S. Reservoir Characterization and Volumetric Analysis of "Lee" Field, Onshore Niger Delta, Using 3D Seismic and Well Log Data. Journal of Applied Science and Environmental Management, 2019; 23(12): 2185-2193.

[7] Short KC, and Stauble AJ. Outline of Geology of Niger Delta. American Association of Petroleum Geologists Bulletin, 1967; 51: 761–779.

[8] Frankl EJ, and Cordy EA. The Niger Delta oil province: Recent developments onshore and offshore. Seventh world petroleum congress proceedings, Mexico, 1967; 2: 195–209.

[9] Avbovbo AA. Tertiary lithostratigraphy of Niger Delta. American Association of Petroleum Geologists Bulletin, Tulsa, Oklahoma, 1978; 96–200.

[10] Reijers TJA. Selected Chapters on Geology: with notes on Sedimentary Geology, Sequence Stratigraphy and three case studies and a field guide. S.P.D.C. Corporate Reprographic Services, Warri, Nigeria, 1996; pp 197.

[11] Obiora DN. Comparative Study of Graphical Methods and Velocity Analysis of 2-D Seismic Reflection Data with Application to Niger Delta. Pacific Journal of Science and Technology, 2006; 7(2): 204-210.

[12] Unukogbon NO, Asuen GO, and Emefurieta WO. Sequence Stratigraphic Appraisal: Coastal Swamp depobelt in the Niger Delta basin, Nigeria. Global Journal of Geological Science, 2008; 6(2): 129-137.

[13] Ejedawe JE, Coker SJL, Lambert-Aikhionbare DO, Alofe KB, and Adoh FO. Evolution of oil-generative window and oil and gas occurrence in Tertiary Niger Delta Basin. American Association of Petroleum Geologists Memoir, 1984; 68: 1744 -1751.

[14] Weber KJ, and Daukoru E. Petroleum geology of the Niger Delta. Proceedings of the Ninth World Petroleum, Congress, 1975; 2: 209–221.

[15] Orife JM, and Avbovbo AA. Stratigraphy and the Unconformity Traps in Niger Delta. American Association of Petroleum Geologist Memoire, 1982; 32(1): 251-265.
[16] Edwards JD, and Santogrossi PA. Summary and conclusions. In: Edwards JD, Santogrossi PA (eds) Divergent and passive margin basins. American Association of Petroleum Geologists Memoir, 1990; 48: 201-238.
[17] Stacher P. Present understanding of the Niger Delta hydrocarbon habitat. In: M. N. Oti, G. Postma, A. A. Rotterdam, A. Balkema (Eds) Geology of Deltas, 1995; pp 257 – 267.
[18] Atlas D (1979) Log interpretation charts. Houston Dresser Industries Inc
[19] Archie GE. The Electrical Resisitivity as an Aid in Determining Some Reservoir Characteristics. Petroleum Transactions of the AIME, 1942; 146(1): 54-62
[20] Asquith G, and Krygowski D (2004) Basic Well Analysis, 2nd Edition. AAPG Methods in Exploration Series.
[21] Timur A. An Investigation of Permeability, Porosity and Residual Water Saturation Relationships for Sandstone Reservoirs. The Log Analyst, 1968; 9(4): 3-5.
[22] Tixier MP. Evaluation of Permeability from Electric Log Resistivity Gradients. Oil and Gas Journal, 1949; 8: 75-90.
[23] Sheriff RE, Geldart LP. Exploration Seismology, Second Edition. Cambridge University Press, 1995; New York, USA, pp150-300.

To whom correspondence should be addressed: Prof. Daniel N. Obiora, Department of Physics and Astronomy, University of Nigeria, Nsukka, Enugu State, Nigeria, E-mail: daniel.obiora@unn.edu.ng